Synthesis of Pyrene-Bearing Oligothiophenes as Novel Light Emitting Materials and Their Application to Single-Organic-Layer Electroluminescence Devices

Yoshio Aso,* Takashi Okai, Yohei Kawaguchi, and Tetsuo Otsubo*
Department of Applied Chemistry, Faculty of Engineering, Hiroshima University, 1-4-1 Kagamiyama, Higashi-Hiroshima 739-8527

(Received January 29, 2001; CL-010087)

Ter- and quaterthiophenes bearing pyrenes at the terminal α or β positions have been synthesized as novel emitting materials in organic electroluminescence devices. The efficient single-layer EL devices of these compounds are fabricated by use of an Al/ultrathin LiF bilayer cathode. One of them exhibits a maximum luminance of 1860 cd/m^2 and a luminous efficiency of 0.15 lm/W, which are of the highest performance class among single-organic-layer EL devices.

It has been recently shown that oligothiophenes can advantageously replace polythiophenes in molecular electronics and optical devices, and some of their physical properties even surpass those of the latter.[1] In fact, oligothiophenes, in analogy with polythiophenes,[2] have been successfully used as active components in organic electroluminescence (EL) devices.[3] However, the efficiency of such devices is generally low, and drastic structural modifications of oligothiophenes thus have been required. It has been demonstrated that extension of oligothiophenes with electron-donating bis(4-methylphenyl)aminophenyl[4] or with electron-withdrawing dimesitylboryl units[5] can produce superior emitting materials with hole- or electron-transport properties in double- and multi-layer EL devices. We have been rather interested in the introduction of fluorescent pyrenes into oligothiophenes in order to enhance their emission properties, highly stable film formation, and high carrier-transport capability. Here we would like to report the synthesis and properties of ter- and quaterthiophenes (**1**, **2**, and **3**) bearing pyrenyl groups at the terminal α or β positions and their application to single-layer EL devices.

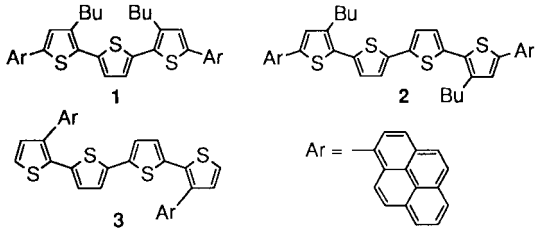

The syntheses of **1**–**3** were carried out using transition metal-catalyzed cross-coupling reactions as illustrated in Scheme 1. The Ni(II)-catalyzed cross-coupling of 2,5-dibromothiophene (**4**) with the Grignard reagent of 2-bromo-3-butylthiophene afforded butyl-substituted terthiophene (**6**) in 72% yield, which was converted to bis(tributylstannyl) derivative (**8**) and then coupled with 1-bromopyrene in the presence of Pd(0) catalyst (Stille coupling) to give **1** in 52% two-step yield. Similarly, **2** was obtained in a good yield starting with 5,5'-dibromobithiophene (**5**). On the other hand, **3** was obtained by Suzuki coupling of 1-bromopyrene with 3-thienylboronic acid (**10**) followed by bromination of the resulting **11** to **12** and finally Stille coupling with bis(tributylstannyl)bithiophene. The compounds **1**–**3** were identified by spectroscopic methods and elemental analysis.[6]

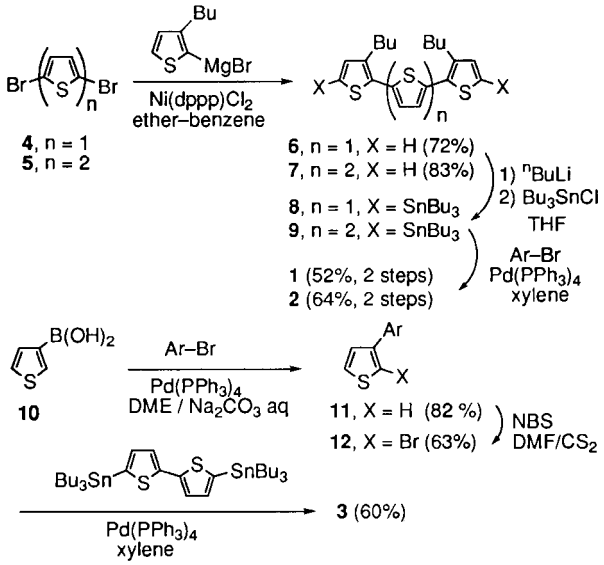

Scheme 1.

Though ter- and quaterthiophenes are known to be inherently crystalline, the pyrene-bearing derivatives **1**–**3** spontaneously formed stable amorphous glasses owing to the introduction of the pyrenyl and/or butyl groups when the melt samples were cooled on standing in air. In the differential scanning calorimetry (DSC) measurements, the crystalline samples of **1** and **2** exhibited two peaks (**1**, 126 and 169 °C; **2**, 116 and 184 °C), which correspond to solid-phase transition and melting process, respectively. On the other hand, **3** demonstrated only a sharp melting peak at a higher temperature (218 °C). The amorphous glassy samples showed a glass transition at 56 °C for **1**, at 65 °C for **2**, and at a much higher temperature 120 °C for **3**. These observations mean that **1**–**3** have the ability to form good quality amorphous films, especially involving a thermally stable film for **3**. As shown in Figure 1, the films of **1** and **2** made by vacuum deposition show almost the same absorption spectra (**1**: λ_{max} 424 nm; **2**: 427 nm), which are notably red-shifted as compared to the parent oligothiophenes, indicating an effective conjugation between the pyrene and oligothiophene moieties. Correspondingly they display intense photoluminescence (PL) in the visible region (**1**: λ_{max} 551 nm; **2**: 598 nm).[7] On the other hand, the absorption spectrum of **3** can be explained by a superposition of the two absorptions due to the pyrene and quaterthiophene chromophores λ_{max} 354 and 419 nm. However, the PL spectrum has only one peak at 552 nm, associated with emission from the quaterthiophene part.

The three pyrene-bearing oligothiophenes (**1**–**3**) were incorporated into EL device structures consisting of a single organic

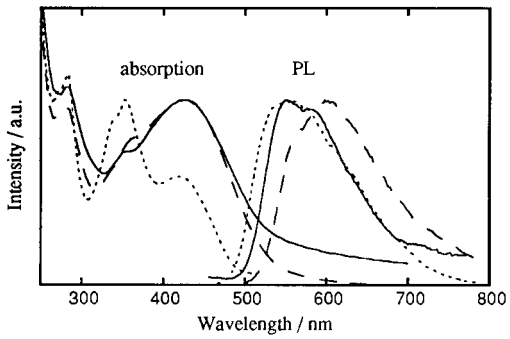

Figure 1. Electronic absorption and photoluminescence spectra of **1** (solid line), **2** (dashed line), and **3** (dotted line) films.

layer between ITO and Al electrodes (ITO/organic layer (100 nm)/Al) by vacuum deposition. Under forward bias, the devices using **1** and **3** worked, and Figure 2 shows the luminance–voltage and current–voltage characteristics for these devices. The device using **1** exhibits a maximum luminance of 14 cd/m^2 at a driving voltage of 16 V, and the device using **3** 73 cd/m^2 at a driving voltage of 9.5 V. However, the luminous efficiencies of these EL devices are very low (2.6×10^{-3} lm/W for **1** and 4.2×10^{-2} lm/W for **3**) owing to relatively large current densities. Although we could not detect any EL signal from a single layer device made of **2**, a similar high current was observed. Considering p-type-semiconducting characteristics of oligothiophenes,[1b] it is suggested that in these devices, hole injection from the anode into the organic layer is much more effective than electron injection from the cathode, and holes injected are efficiently transported to the counter electrode.

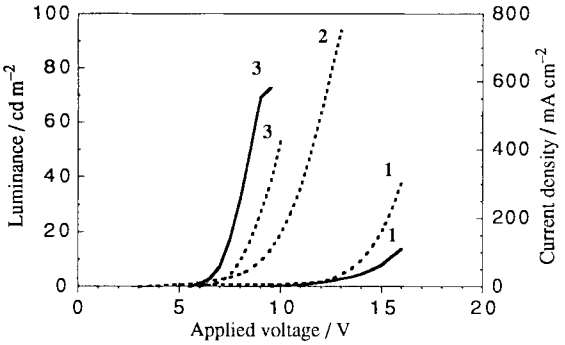

Figure 2. Luminance (solid lines) and current density (dotted lines) vs applied voltage profiles of single layer EL devices using **1**, **2**, and **3**.

Hung and coworkers recently reported that an Al/LiF bilayer electrode enhances electron injection as compared to an Al electrode itself,[8] so we applied such a bilayer electrode to the present single-organic-layer EL devices. All the bilayer-cathode devices using **1**–**3** (ITO/organic layer (100 nm)/LiF (0.6 nm)/Al) emitted visible light (**1**: yellow, **2**: orange, and **3**: green), and their EL spectra has close resemblance to the corresponding PL spectra. As demonstrated in Figure 3, the EL performances are extremely improved as compared to those of the above single-cathode EL devices. In particular, the device using **1** exhibited a maximum luminance of 1860 cd/m^2 at a driving voltage of 12.5 V and a maximum luminous efficiency of 0.15 lm/W, which are of the highest performance class among single-organic-layer EL devices. Obviously, use of an Al/ultrathin LiF bilayer electrode serves to

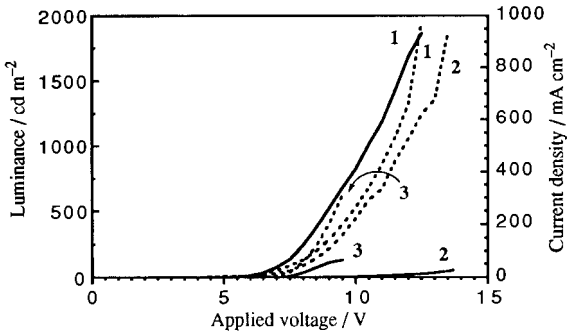

Figure 3. Luminance (solid lines) and current density (dotted lines) vs applied voltage profiles of bilayer-cathode EL devices using **1**, **2**, and **3**.

enhance electron injection to balance with hole injection. However, it is difficult to rule out the possibility that the insulating LiF layer also functions as a hole transport block. Anyhow, the present results demonstrate that the Al/ultrathin LiF bilayer cathode is very useful for single-organic-layer EL devices using p-type-semiconductor emitting materials.

References and Notes

1 a) "Polythiophenes–Electrically Conductive Polymers," ed. by G. Schopf and G. Koβmehl, Springer, Berlin (1997). b) "Handbook of Oligo- and Polythiophenes," ed. by D. Fichou, Wiley-VCH, Weinheim (1999).

2 a) Y. Ohmori, M. Uchida, K. Muro, and K. Yoshino, *Jpn. J. Appl. Phys.*, **30**, L1938 (1991). b) D. Braun, G. Gustafsson, D. McBranch, and A. J. Heeger, *J. Appl. Phys.*, **72**, 564 (1992). c) M. Berggren, O. Inganäs, G. Gustafsson, J. Rasmusson, M. R. Andersson, T. Hjertberg, and O. Wennerström, *Nature*, **372**, 444 (1994). d) M. R. Andersson, M. Berggren, O. Inganäs, G. Gustafsson, J. C. Gustaffson-Carlberg, D. Selse, T. Hjertberg, and O. Wennerström, *Macromolecules*, **28**, 7525 (1995). e) M. Granström and O Inganäs, *Appl. Phys. Lett.*, **68**, 147 (1996).

3 a) F. Geiger, M. Stoldt, H. Schweizer, P. Bäuerle, and E. Umbach, *Adv. Mater.*, **5**, 922 (1993). b) K. Uchiyama, H. Akimichi, S. Hotta, H. Noga, and H. Sasaki, *Synth. Met.*, **63**, 57 (1994). c) G. Horowitz, P. Delannoy, H. Bouchriha, F. Deloffre, J.-L. Fave, F. Garnier, R. Hajlaoui, M. Heyman, F. Kouki, P. Valat, V. Wintgens, and A. Yassar, *Adv. Mater.*, **6**, 752 (1994). d) M. Muccini, R. F. Mahrt, R. Henning, U. Lemmer, H. Bässler, F. Biscarini, R. Zamboni, and C. Taliani, *Chem. Phys. Lett.*, **242**, 207 (1995). e) C. Väterlein, H. Neureiter, W. Gebauer, B. Ziegler, M. Sokolowski, P. Bäuerle, and E. Umbach, *J. Appl. Phys.*, **82**, 3003 (1997).

4 a) T. Noda, I. Imae, N. Noma, and Y. Shirota, *Adv. Mater.*, **9**, 239 (1997). b) T. Noda, H. Ogawa, N. Noma, and Y. Shirota, *Appl. Phys. Lett.*, **70**, 699 (1997). c) T. Noda, H. Ogawa, N. Noma, and Y. Shirota, *Adv. Mater.*, **9**, 720 (1997). d) T. Noda, H. Ogawa, N. Noma, and Y. Shirota, *J. Mater. Chem.*, **9**, 2177 (1999).

5 a) T. Noda and Y. Shirota, *J. Am. Chem. Soc.*, **120**, 9714 (1998). b) T. Noda, H. Ogawa, and Y. Shirota, *Adv. Mater.*, **11**, 283 (1999).

6 Selective physical and spectral data of **1**: orange fine crystals from hexane/chloroform (10:1 v/v); mp 178–180 °C; ^{1}H NMR ($CDCl_3$) δ 8.64 (d, J = 9.4 Hz, 2H), 8.22–8.02 (m, 16H), 7.26 (s, 2H), 7.24 (s, 2H), 2.97 (t, J = 7.8 Hz, 4H), 1.81 (m, 4H), 1.81 (sext, J = 7.4 Hz, 4H), 1.02 (t, J = 7.4 Hz, 6H); FABMS m/z 760 (M^+). **2**: red fine crystals from chloroform/hexane (1:2 v/v); mp 197–198 °C; ^{1}H NMR ($CDCl_3$) δ 8.63 (d, J = 9.4 Hz, 2H), 8.22–8.01 (m, 16H), 7.25 (s, 2H), 7.22 (d, J = 3.8 Hz, 2H), 7.17 (d, J = 3.8 Hz, 2H), 2.95 (t, J = 7.9 Hz, 4H), 1.80 (m, 4H), 1.53 (sext, J = 7.3 Hz, 4H), 1.02 (t, J = 7.3 Hz, 6H); FABMS m/z 842 (M^+). **3**: orange fine crystals from dichloromethane/hexane (2:1 v/v); mp 245–247 °C; ^{1}H NMR ($CDCl_3$) δ 8.19–7.83 (m, 18H), 7.32 (d, J = 5.1 Hz, 2H), 7.08 (d, J = 5.1 Hz, 2H), 6.44 (d, J = 4.0 Hz, 2H), 6.35 (d, J = 4.0 Hz, 2H); FABMS m/z 730 (M^+).

7 The fluorescence quantum yields of **1**, **2**, and **3** in chloroform are 0.36 (λ_{max} at 534 nm), 0.41 (543 nm), and 0.15 (513 nm), respectively.

8 L. S. Hung, C. W. Tang, and M. G. Mason, *App. Phys. Lett.*, **70**, 152 (1997).